

# Array-Based Split-Pool Combinatorial Screening of Potential Catalysts

Matthew L. Stanton and James A. Holcombe\*

*Department of Chemistry and Biochemistry, University of Texas at Austin, Austin, Texas 78712*

*Received August 25, 2006*

A new method for screening split-pool combinatorial libraries for catalytic activity is described. Site-selective detection of catalytic activity for solution-based reactions was made possible without cofunctionalizing beads or adding diffusion-limiting matrixes. This was done by spatially separating resin-bound catalysts on an adhesive array on a microscope slide and introducing the reacting liquid to the top of the slide. Convective mixing and evaporation was controlled using a cover slide and imaging both the formation of products within active beads and the diffusion of products out of the beads. Colored reaction products and pH-sensitive indicators were used to visually detect catalytically active beads in the presence of inactive ones. Quantitative analyses of the images support the assumption that color intensities can be used to assess the quality of hits from a combinatorial screen. The Knoevenagel condensation reaction catalysis as well as esterase screening using methyl red were used to validate the approach. Using the esterase data, it was shown that some information on activity could also be extracted from the colored plume surrounding individual beads although the precision is not as good as that from direct measurement of absorbance through the bead. It was also found that the distribution of products within a single bead can also be gleaned from the absorbance data for different-sized beads.

## Introduction

The use of split-pool combinatorial libraries for catalyst development is growing in importance.<sup>1–4</sup> Split-pool combinatorial chemistry allows one to synthesize large numbers of potential catalysts which can then be screened to find catalytic structures that may go undiscovered with other methodologies. Screening pooled libraries for catalytic activity is complicated by the fact that the catalyst centers remain unchanged, and as a reaction progresses, products diffuse away from the bead-bound catalysts, thus compromising the selection of active members from a library. Methods that account for this have been developed, whereby the site-selective detection of catalytic activity is facilitated by adding bead-bound indicators<sup>5–8</sup> or by hindering the diffusion of products away from the active beads.<sup>9–11</sup> Unfortunately, these methods can limit the type of reactions that can be screened, and they often add procedural complexities that are ideally avoided. As a result, new and improved methods that broaden the range of applicable reactions without adding excess complications are sought.

Spectroscopic screening techniques on arrayed libraries have been previously used to discover active catalysts.<sup>12–14</sup> The method described in this paper simplifies and enhances the robustness of the screening process by allowing freely diffusible products to develop within a solution without requiring gels or bead-bound indicators. This method operates by spatially separating the beads using a commercial adhesive array and then performing the reaction on the array using a cover slide to limit convection and evaporation, thereby allowing reaction products to diffuse in a controlled and

observable manner. As the reaction progresses, the products increase in concentration in and around the catalytically active beads, and these localized areas of higher product concentration can be detected through visible absorption and most likely other methods such as IR thermography and fluorescence. This allows the simultaneous site-selective detection of catalytically active beads without the inherent limitations associated with other methods.

## Experimental Details

**Catalytic Knoevenagel Condensation Screening.** Unmodified Wang resin 100–200 mesh (Novabiochem) was mixed with piperazinomethyl polystyrene **1** (Novabiochem) in a 5:1 mass ratio. To ensure dryness, beads were exposed to a steady stream of nitrogen gas for several hours at room temperature. The mixed beads were placed on a 7.5 cm × 2.5 cm Tacky Dot slide (SPI Supplies) containing adhesive spots 75 μm in diameter with columns and rows spaced 500 μm apart. The beads were then gently shaken to spread the beads out across the slide. For the reactions with ethyl cyanoacetate, the loaded slides were placed in the water of a sonicator for <1 s to remove clumped beads. The plate was then air-dried for 15 min.

A solution of 3 mmol malononitrile 98% **2** (Acros) or 3 mmol of ethyl cyanoacetate 99% **3** (Acros) in 2 mL acetonitrile optima (Fisher) was made. To this solution, 0.1 mmol 1-pyrenecarboxaldehyde 99% **4** (Aldrich) was added to create a clear yellow solution in both cases. The plate containing immobilized noncatalytic and catalytic beads in a 5:1 ratio was placed on the microscope stage, and 250 μL of one of the above solutions was pipetted onto the plate. A full-size microscope slide was used as a cover slide and was immediately pressed on top of the Tacky Dot slide. Even

\* Author to whom correspondence should be directed. E-mail: holcombe@mail.utexas.edu.

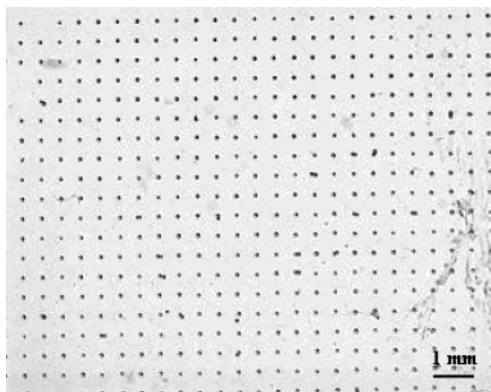


**Figure 1.** Immobilized beads on adhesive array.

pressure was applied to form an even layer of solution across the slide. The 250  $\mu\text{L}$  portion of the reagent solution was enough to cover the slide area once the cover slide was applied, and no clamps were used to hold the cover slide in place. Appropriate safety precautions should be observed when handling the prepared slide, as the cover slide does not eliminate evaporation and dangerous gases may be released depending on the reaction.

The reaction was monitored by imaging the array approximately every minute, and at the end of the reaction, the active beads were removed with tweezers using the grid coordinates in the images as a guide. For ease of preparation, an entire Tacky Dot slide was used for each screen even though the entire dot area was not necessarily screened. Additional screens using only **1** or unmodified Wang resin were performed using the same procedure.

Imaging was performed with a DVC 1312C-FW-TE color camera equipped with a  $\frac{2}{3}$  in. Sony ICX085AK charge-coupled device (CCD). Samples were illuminated from beneath using white light. Images were captured using DVCView (DVC Co.). Prior to beginning the reactions, the white balance was autoadjusted with the bead-loaded plate and cover slide in view. Various optical magnification settings were used to give image areas of 13 mm  $\times$  10 mm, 9 mm  $\times$  7 mm, and 2.25 mm  $\times$  1.17 mm. While the higher magnifications were useful for examining the screening process, the 13 mm  $\times$  10 mm magnification gave enough resolution (Figure 1) to detect catalytically active beads and should be suitable for screening purposes.

To obtain quantitative data, the plate images were loaded into ImageJ (NIH) and processed as follows: RGB images were split, and the blue pixels were used for analysis. A rolling ball background subtraction was applied to flatten the illumination, and the image was inverted. A threshold was applied to the inverted image with the lower threshold set to  $3\sigma$  above the background and no upper threshold. The beads were autoanalyzed using the Analyze Particles command, with the particle size set to 200 pixels<sup>2</sup>–infinity and the circularity set to 0.3–1.0. Included in the analysis table were area and integrated density values.

**Esterase Screening using Methyl Red.** Porcine liver esterase (PLE) was immobilized using a method developed by Lauman et al.,<sup>15</sup> and the esterase-bound beads **5** were stored at 7  $^{\circ}\text{C}$  in a 1 M phosphate buffer containing 0.03% sodium azide.

Beads were removed from the buffered storage solution using gravity filtration, followed by 3 20 mL washes of water. The beads were dried using a steady stream of nitrogen for no more than 5 min. Unmodified Eupergit C acrylic beads were then mixed with **5** in a 30:1 mass ratio. The mixed beads were loaded onto a Tacky Dot slide (SPI Supplies), and the slide was sonicated for  $\sim 0.5$  s to remove clumped beads. Immediately after immobilizing the beads, 250  $\mu\text{L}$  of 0.4 M ethyl acetate **6** (Acros) and 0.2 mM methyl red sodium salt **7** (Acros) prepared in deionized water (pH 6.2) was pipetted onto the array. A cover slide was pressed on top, and the slide was imaged as before.

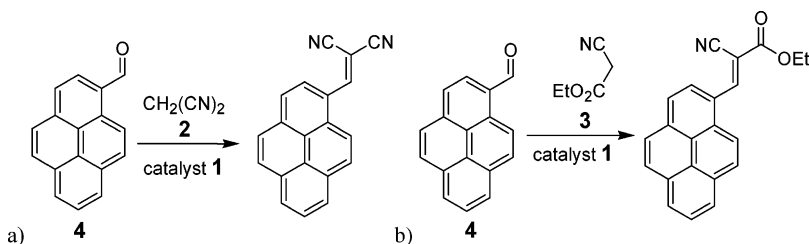
For quantitative analysis, RGB images were split and the blue pixels were used for analysis. To obtain background intensity values, several line scans in the vicinity of each bead of interest were taken, the background values were averaged, and the variance was determined. The background intensities were used to determine the start of the product plume, which began at the point that the grayscale intensity dropped to  $6\sigma$  below the background.

## Results and Discussion

**Array-Based Screening.** The array-based screen allows split-pool combinatorial libraries to be screened for catalytic activity in solution without the need for insoluble products, cofunctionalized beads, or diffusion-limiting gel matrixes. This screen employs an adhesive array to form an ordered arrangement of over 3000 beads in less than 1 min. Figure 1 shows the spatial separation achieved on a part of the Tacky Dot slide. To properly adhere the beads to the plate, the beads must be free flowing, which can be accomplished by drying the beads under a stream of nitrogen if the beads are stored wet. Once the beads are loaded onto the slide, the reagent solution is added via pipet and a cover slide is pressed on top. The cover slide is necessary to control the diffusion of reaction products by eliminating convection from air currents and evaporation. The reaction is then imaged over time to monitor the buildup of products forming within and diffusing out of the catalytically active beads. In this study, the products were detected colorimetrically, although it is likely that other detection methods (e.g., fluorescence, IR thermography) could be used. Once the reaction has progressed, the images are used to locate the grid coordinates of the active catalysts, and the beads of interest can be manually removed for structural analysis (e.g., Edman degradation). Although not performed here, physically locating the bead on the plate could be facilitated by adding registration marks to each slide, which would help in matching slide areas with their corresponding images.

To test the effectiveness of this combinatorial screen, the Knoevenagel condensations of **4** with **2** (Scheme 1a) and **3** (Scheme 1b) were performed in the presence of catalyst-bound and unmodified beads. These reactions made good test reactions because they form freely diffusible products that can be detected visually. Johansson and co-workers used these reactions to test their gel-based combinatorial screen,<sup>10</sup> and it was of interest to see if the array-based screen could facilitate site-selective detection of catalytically active beads without adding the complexities of a gel.

**Scheme 1.** Catalytic Knoevenagel Condensation of 1-Pyrenecarboxaldehyde with (a) Malononitrile and (b) Ethyl Cyanoacetate



For the reaction of **2** (Scheme 1a), within the first minute, the active beads took on a yellow color that became darker as the reaction progressed. After 2 min, a colored diffusion plume around the active beads became visible, and the catalytically active beads became clearly distinguishable from inactive ones. As time progressed, the products became more concentrated, and the active beads took on a dark red color surrounded by a slowly enlarging yellow product plume (Figure 2a–c). After 15 min, the inactive beads surrounding the active ones had turned yellow due to products diffusing into those beads, but the difference in product concentrations between the active and inactive beads remained clearly distinguishable (Figure 2d). If diffusion overlap becomes a problem for a particular reaction, simply switching to an array with greater spacing should solve the issue (although this will reduce throughput). After the reaction had progressed, the cover slide was removed, and the active beads were easily selected with tweezers from the array using grid coordinates from the images as a guide.

The buildup of products from the condensation of **3** also allowed the site-selective detection of active beads. Yellow

products became faintly visible within the active beads at 3 min, and at 20 min, the active beads took on a darker yellow color and were clearly distinguishable from the inactive ones (Figure 3a–d). The product plume for this reaction was not detectable, which was most likely due to a slower rate of product formation and a smaller difference in absorbance between the reactants and the products. After 20 min, it was easy to determine which beads were catalytically active, and these beads were removed from the array as before.

There was some question as to whether the colored beads seen in the previous screens were indeed **1**. To test this, plates loaded with 0% active beads and 100% active beads were screened using the reaction with **3**. After 20 min, the plate containing no catalytically active beads showed no color change (Figure 4a), while the plate containing all active beads produced a color change within and around each bead (Figure 4b). This supports the assumption that **1** was the cause the color change and that the inert beads had no participation in the reaction.

Although it had previously been reported that beads free in solution compromised site-selective detection,<sup>10,11</sup> it was

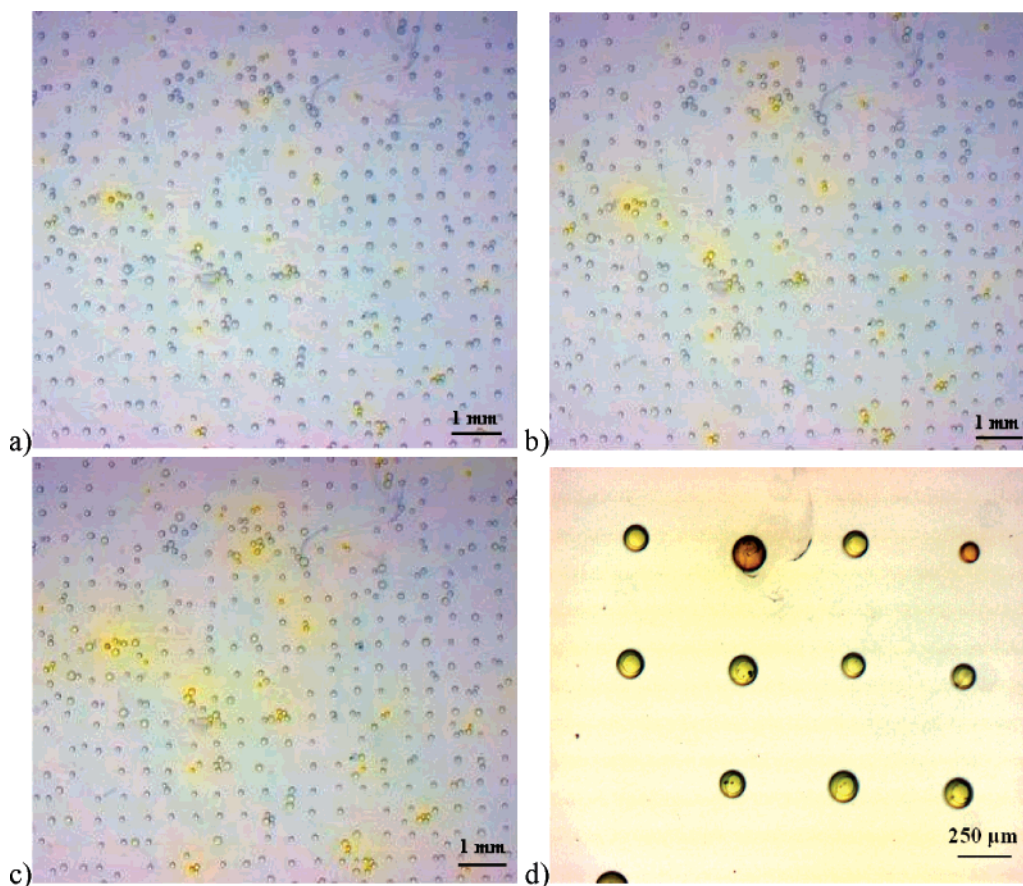


**Figure 2.** Reaction progression with malononitrile: (a) 2 min, (b) 4 min, (c) 7 min, (d) optical zoom at 15 min.

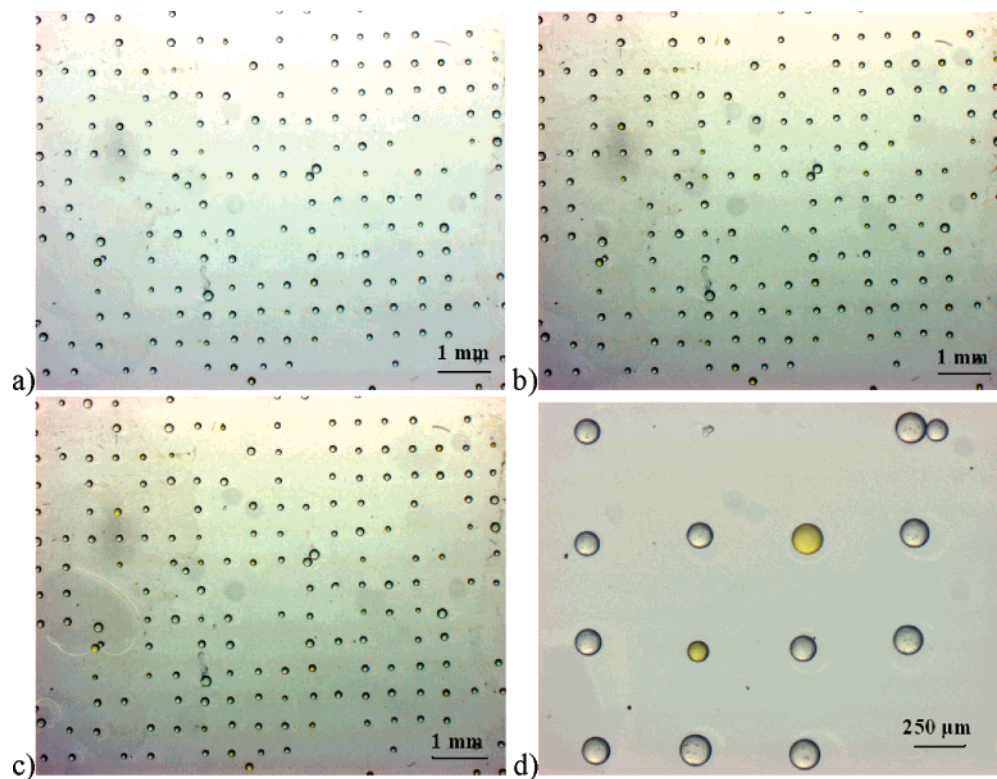


**Figure 3.** Reaction progression with Ethyl cyanoacetate: (a) 3 min, (b) 7 min, (c) 20 min, (d) optical zoom at 20 min.

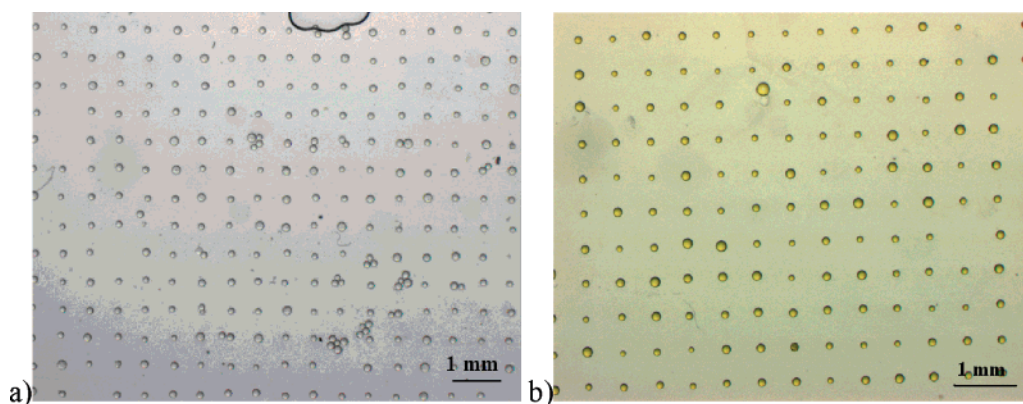


**Figure 4.** Condensation reactions with ethyl cyanoacetate after 20 min with (a) 0% active and (b) 100% active beads.

still necessary to affirm that the array was a requirement for this method. To do this, the condensation of **3** was performed on a group of active and inactive beads (1:5 ratio) in a vial without the array. As expected, the mixing of colored products made it impossible to select the catalytically active beads from the inactive ones (Figure 5).

This work matched the results that Johansson and co-workers achieved by performing these reactions in gels.<sup>10</sup> Thus, by using an array and imaging the product formation during the reaction, the complexities associated with the gel were eliminated while still allowing the site-selective detection of catalytic activity.

**pH-Sensitive Indicators.** The previous reactions demonstrated that the array-based combinatorial screen could be utilized for reactions that produce a diffusible colored product. To demonstrate that a broader range of reactions could be compatible with this method, a reaction that produces a pH change but no colored products was screened by adding a pH-sensitive indicator to the reagent solution.

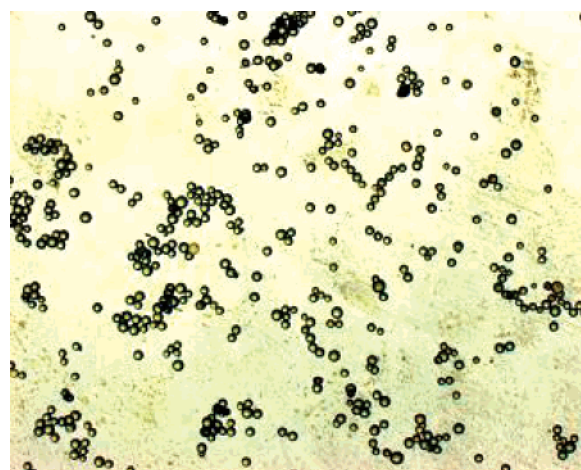


**Figure 5.** Imaging without an array using the cyanoacetate condensation reaction.

Müller and co-workers also faced this challenge for their gel-based combinatorial screen.<sup>11</sup> To broaden the scope of

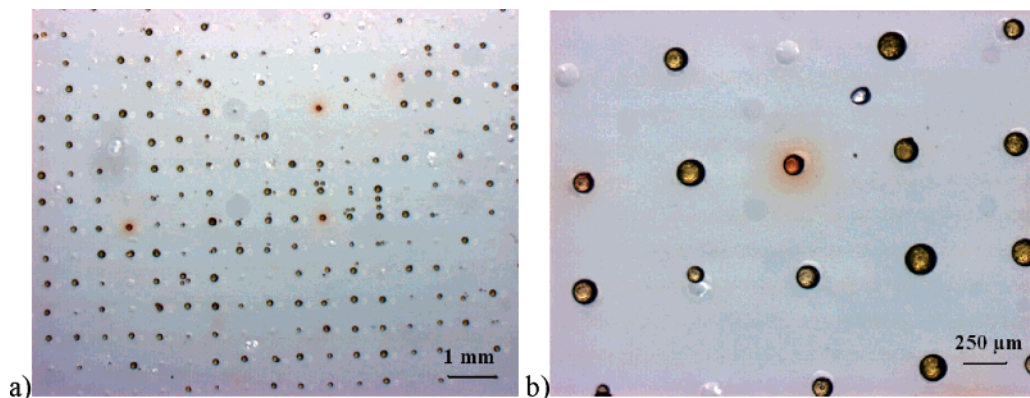
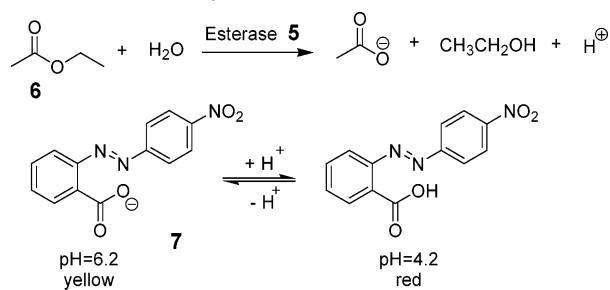


**Figure 6.** Esterase screen at 10 min using protonated methyl red for site-selective detection: (a) full view, (b) optical zoom.

**Scheme 2.** Esterase-Catalyzed Hydrolysis of Ethyl Acetate in the Presence of Methyl Red



their method, **7**, a pH-sensitive colored indicator, was employed to screen esterase reactions that cause a pH change. This strategy proved effective, and the pH-sensitive indicator coupled with gel-based screening provided the site-selective detection of active catalysts by detecting localized changes in pH around the catalytically active beads. Building off this research, it was thought that a colored indicator would be compatible with the array-based screening, thus it would be possible to screen reactions that do not produce colored products.

To test if colored indicators would facilitate site-selective detection of catalytic activity in the array-based screen, **7** was used to detect the ester hydrolysis of **6** catalyzed by **5** in the presence of inactive beads in a 1:30 ratio (Scheme 2).

To screen this reaction, the esterase-loaded beads were dried for 5 min (longer drying times diminished the activity of the enzyme) before mixing with inactive beads and loading on the Tacky Dot slide. At the start of the reaction, the reagent solution (pH 6.2) was yellow in color due to the unprotonated form of **7** in solution. As the reaction progressed for several minutes, some of the beads in the array took on a red color and a plume of red products could be seen diffusing out from the catalytically active beads. The red color is due to the formation of protonated **7** which concentrates in and around the active beads. Figure 6 shows an image of the esterase screen at 10 min, where three catalytically active beads are distinguishable from the surrounding inactive beads. This reaction shows that pH-sensitive indicators can be combined with the array-based screening to provide the site-selective detection of catalytic activity.

To ensure that the array was necessary, the reaction was run without the array by reacting a mix of active and inactive

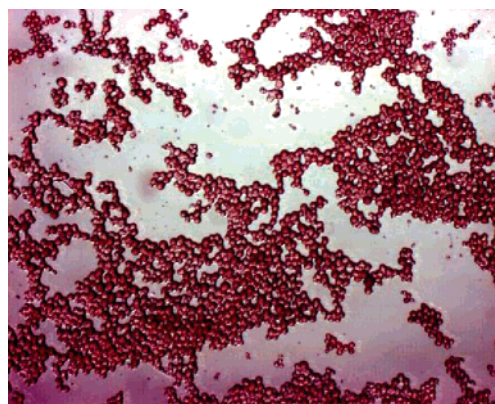


**Figure 7.** Mix of active and inactive beads reacted together in a vial.

beads (1:20 ratio) together in a vial for 30 min. As expected, the site-selective detection of inactive beads was compromised due to mixing and uncontrolled diffusion of reaction products (Figure 7).

**Quantification of In-Bead Product Formation.** While most literature sources simply assume that darker colors from the images of catalytic screens correspond to the best catalysts, little quantitative work has been performed to determine how well the quality of a hit can be assessed. To determine this, the on-bead intensity values from the ethyl cyanoacetate condensation screen were studied. Images from the screen of 100% active beads were used to determine the amount of variance between averaged bead intensities. The statistical difference between the intensities of active and inactive beads was then analyzed to establish how well the quality of a hit could be assessed.

Using the background-corrected and inverted images from the ethyl cyanoacetate screen with 100% active beads (Figure 8a), the average inverted intensity values of the beads were compared. Because all the beads contained the same catalyst and they were all exposed to the same reactions conditions, the average inverted intensity (which corresponds to the average absorbance) of each bead was expected to be the same. The sum of the inverted intensities of each bead (i.e., inverted integrated density) was normalized by bead area, because the products did not have time to diffuse evenly throughout the bead at time 20 min. As a result, only a layer around the periphery of the bead contained products, and this layer's thickness was independent of bead size. In assessing the extent of color change, the edges of the bead

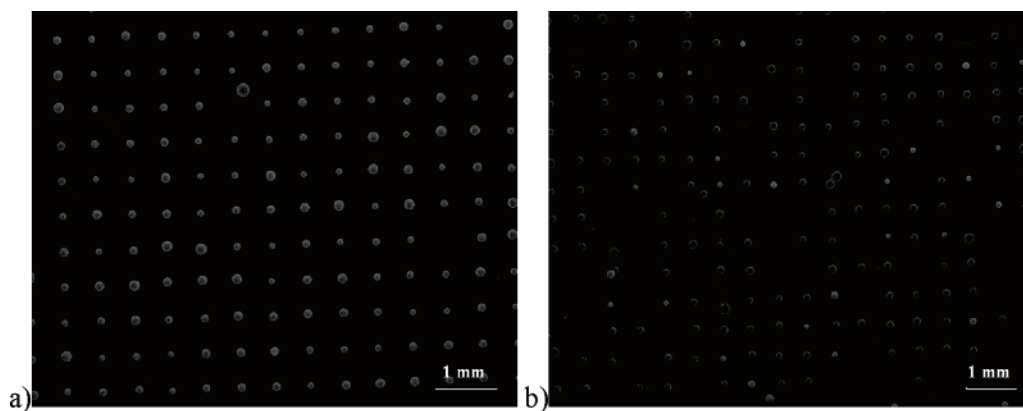


**Figure 8.** Inverted background-corrected images for the ethyl cyanoacetate condensation: (a) 100% active beads, (b) 5:1 inactive-to-active bead mixture.

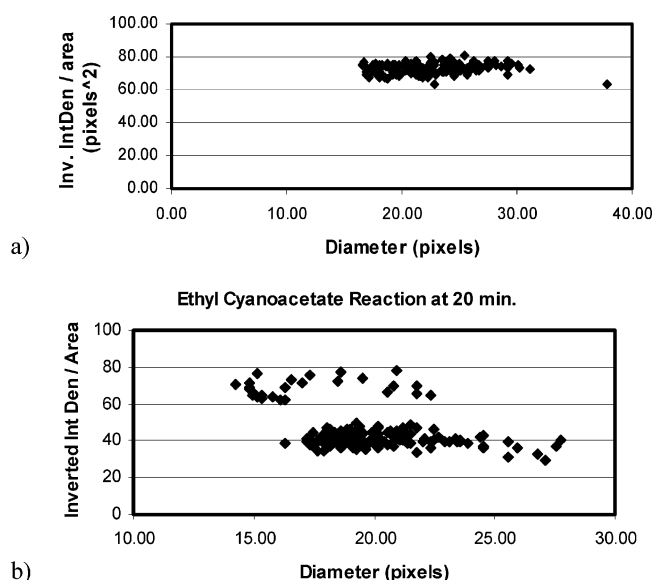


**Figure 9.** (a) Comparison of all active beads of varying sizes normalized area. (b) Average absorbance comparison of active and inactive beads for the ethyl cyanoacetate condensation screen at 20 min.

were avoided due to refractive optical effects in these regions. The inverted integrated densities normalized by area seen in Figure 9a show similar absorbances ( $\pm 4\%$ ) across the beads regardless of size. This low amount of variation confirms that the integrated densities should be averaged by area to account for the bead size.

The statistical difference between active and inactive beads for the ethyl cyanoacetate condensation was then determined. An image at 20 min from the 1:5 active-to-inactive bead mixture screen was analyzed to generate the inverted integrated density values normalized by area. Figure 9b shows a graph comparing the dependence of average inverted integrated densities on bead size. A clear separation between the active and inactive beads exists along the y-axis, with the catalytically active beads at higher average inverted integrated densities (i.e., greater absorbance) than the inactive beads. The active bead's normalized inverted integrated densities average to 70 with a relative standard deviation (RSD) of 7%, while the inactive beads average to 41 with an RSD of 11%. These numbers show a statistically significant separation between the active and inactive beads.

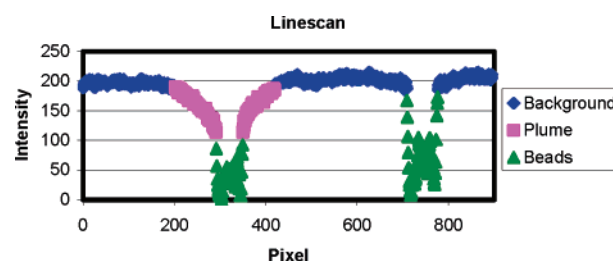


**Figure 10.** Line scan across an active bead with a product diffusion plume and an inactive bead.

The purpose of doing this analysis was to determine how well hit quality could be assessed from an actual combinatorial library where the members of a library exhibit varying degrees of catalytic ability. This data suggests that absorbance changes of 10–20% may be only marginally distinguishable based on criteria of statistical significance. However, the variance is small enough that larger differences in absorbance can be attributed to real differences in catalytic ability. Thus, this screen should work well as a broad screen that can quickly remove the vast majority of potential catalysts from a large split-pool combinatorial library. The remaining beads of interest can then be subjected to more detailed analytical tests to get firm numbers on their catalytic strength.

**Quantification of the Product Plume.** An analysis of the light intensities from the diffusion plume of the esterase reaction was performed to determine the variability among plume intensities of identical catalysts. While the variance between like beads was acceptable, analyzing the signal within the bead is not simple. Optical interferences are unavoidable due to the spherical shape of the beads, and these aberrations cause shadowing that is difficult to accurately subtract out. To avoid taking measurements through the sphere, it was suggested that measurements be taken at a fixed distance away from the bead in the product plume.

Figure 10 shows a line scan that transverses an active and an inactive bead. The graph shows the intensity values of the background, plume, and beads, with the plume defined as nonbead pixels that have a signal intensity of at least  $3\sigma$  above the background. Since the intensity values of the product plume showed a statistically significant separation from the background, it was determined that the product plume could be subjected to more thorough quantitative analysis.

Because the catalytically active beads in the esterase screen were composed of the same catalyst under the same conditions, the product plume intensities should be similar across multiple beads. Plume intensities at a fixed distance away from the bead could not be compared across beads of varying size, because it was determined that the plume sizes (thus the plume intensities at a given distance from the bead) were influenced by the size of the bead. Since the plume sizes could be normalized using the bead sizes, intensity measurements were taken at a distance determined by each bead's size to compare intensity measurements across different beads. A distance away from the edge of the bead at  $1/4$  of the diameter of the bead was used as the point for measuring plume intensities. This distance was used so that the measured intensities would be well within the plume but clearly separated from the edge of the bead.

Using this calculated distance for measurements, the intensities from the plumes of several beads were compared to give an RSD of 10%. This variation between intensities showed that examining the product plume does not give more precise measurements than analyzing the intensities through the bead. It is possible that convection caused by slight disturbances from positioning the slide or evaporation along the edges of the slide can disrupt the symmetrical diffusion of the product plume. This evaporation coupled with slight movements required for imaging multiple areas may impact the variance in the product plumes. If a 10% RSD is too much error to distinguish quality hits in a combinatorial screen, then adjustments to the system will need to be made if the product plume is to be used to assess the quality of hits. To limit the disturbance of the product plume, it is recommended that the slide stay stationary and the camera be moved to image multiple areas. In addition, a cover that completely seals the sides of the slide would eliminate evaporation and may improve the analysis of the product plume.

### Conclusions

A robust and effective screen for catalyst development has been developed without the inherent limitations or complexities associated with other methods. These experiments show that the spatial separation of resin-bound catalysts, coupled with the imaging of controlled product diffusion, can be used to identify active catalysts from a pool of active and inactive beads without the need for bead-bound indicators or diffusion-limiting gels. A visible absorption difference between the products and reactants was used to site-selectively detect product formation in and around the catalytic beads. These experiments showed that pH-sensitive indicators can be used with the array-based screening method to screen reactions that produce colorless products. This expands the range of reactions that can be screened, and it is expected that other detection methods such as fluorescence and IR thermography should be compatible with the array-based screen. Quantitative studies showed that statistically significant differences in absorbance exist between catalytic and noncatalytic beads,

and either the light intensity within the bead or in the product plume can be used to assess the quality of hits in a screen.

**Acknowledgment.** This work was supported, in part, by a grant from the Robert A. Welch Foundation.

### References and Notes

- (1) Berkessel, A. The Discovery of Catalytically Active Peptides Through Combinatorial Chemistry. *Curr. Opin. Chem. Biol.* **2003**, *7*, 409–419.
- (2) Fonseca, M. H.; List, B. Combinatorial chemistry and high-throughput screening for the discovery of organocatalysts. *Curr. Opin. Chem. Biol.* **2004**, *8* (3), 319–326.
- (3) Wennemers, H. Combinatorial chemistry: A tool for the discovery of new catalysts. *Comb. Chem. High Throughput Screening* **2001**, *4* (3), 273–285.
- (4) Woo, S. I.; Kim, K. W.; Cho, H. Y.; Oh, K. S.; Jeon, M. K.; Tarte, N. H.; Kim, T. S.; Mahmood, A. Current Status of Combinatorial and High-Throughput Methods for Discovering New Materials and Catalysts. *QSAR Comb. Sci.* **2005**, *24* (1), 138–154.
- (5) Evans, C. A.; Miller, S. J. Proton-activated fluorescence as a tool for simultaneous screening of combinatorial chemical reactions. *Curr. Opin. Chem. Biol.* **2002**, *6* (3), 333–338.
- (6) Copeland, G. T.; Miller, S. J. A Chemosensor-Based Approach to Catalyst Discovery in Solution and on Solid Support. *J. Am. Chem. Soc.* **1999**, *121* (17), 4306–4307.
- (7) Copeland, G. T.; Miller, S. J. Selection of Enantioselective Acyl Transfer Catalysts from a Pooled Peptide Library through a Fluorescence-Based Activity Assay: An Approach to Kinetic Resolution of Secondary Alcohols of Broad Structural Scope. *J. Am. Chem. Soc.* **2001**, *123* (27), 6496–6502.
- (8) Krattiger, P.; McCarthy, C.; Pfaltz, A.; Wennemers, H. Catalyst-substrate coimmobilization: A strategy for catalysts discovery in split-and-mix libraries. *Angew. Chem., Int. Ed.* **2003**, *42* (15), 1722–1724.
- (9) Harris, R. F.; Nation, A. J.; Copeland, G. T.; Miller, S. J. A Polymeric and Fluorescent Gel for Combinatorial Screening of Catalysts. *J. Am. Chem. Soc.* **2000**, *122* (45), 11270–11271.
- (10) Johansson, K.-J.; Andrae, M. R. M.; Berkessel, A.; Davis, A. P. Organogel media for on-bead screening in combinatorial catalysis. *Tetrahedron Lett.* **2005**, *46* (22), 3923–3926.
- (11) Müller, M.; Mathers, T. W.; Davis, A. P. A new screen for combinatorial catalysis; on-bead testing in agarose gel. *Angew. Chem., Int. Ed.* **2001**, *40* (20), 3813–3815.
- (12) Miller, T. C.; Mann, G.; Havrilla, G. J.; Wells, C. A.; Warner, B. P.; Baker, R. T. Micro-X-ray Fluorescence as a General High-Throughput Screening Method for Catalyst Discovery and Small Molecule Recognition. *J. Comb. Chem.* **2003**, *5* (3), 245–252.
- (13) Dai, Q. X.; Xiao, H. Y.; Li, W. S.; Na, Y. Q.; Zhou, X. P. Photodegradation Catalyst Discovery by High-Throughput Experiment. *J. Comb. Chem.* **2005**, *7* (4), 539–545.
- (14) Garbacia, S.; Touzani, R.; Lavastre, O. Image Analysis as a Quantitative Screening Test in Combinatorial Catalysis: Discovery of an Unexpected Ruthenium-Based Catalyst for the Sonogashira Reaction. *J. Comb. Chem.* **2004**, *6* (3), 297–300.
- (15) Laumen, K.; Reimerdes, E. H.; Schneider, M.; Goerisch, H. Hydrolytic enzymes in organic synthesis. 5. Immobilized porcine liver esterase: a convenient reagent for the preparation of chiral building blocks. *Tetrahedron Lett.* **1985**, *26* (4), 407–10.